Int. J. Electrochem. Sci., 16 **(2021)** 150962, doi: 10.20964/2021.01.16

International Journal of
ELECTROCHEMICAL
SCIENCE
www.electrochemsci.org

Review

Electrodeposition of Ni-Co Film: A Review

Inam M.A. Omar[1,2], *Khadijah M. Emran*[3,*], *Madzlan Aziz*[4]

[1] Chemistry Department, College of Science, Taibah University, AlMaddinah Al Mounwara, SAUDI ARABIA.
[2] Department of Chemistry, Faculty of Science, Universiti Teknologi Malaysia, 81310 Johor Bahru, Johor, MALAYSIA.
[3] Chemistry Department, College of Science, Taibah University, AlMaddinah Al Mounwara, SAUDI ARABIA
[4] Department of Chemistry, Faculty of Science, Universiti Teknologi Malaysia, 81310 Johor Bahru, Johor, MALAYSIA.
[*]E-mail: kabdalsamad@taibahu.edu.sa

Received: 25 September 2020 / *Accepted:* 3 November 2020 / *Published:* 30 November 2020

Nickel (Ni), cobalt (Co) and their alloy have been extensively employed in engineering due to their magnetic, chemical, mechanical, physical and electrocatalytic characteristics, which grant resistance against corrosion and heat. Electrodeposition is considered to be a significant and environmentally friendly technique for producing Ni, Co and their alloy coatings due to its promising properties. The current research provides a brief review of the latest studies of different types of Ni, Co, and Ni-Co alloy electrodeposition from different aqueous baths. This article reviews the effects of various organic additives in Ni, Co and their alloy electrodeposition processes. Due to the special functions of organic additives, they are widely used during electrodeposition. The additives usually affect the growth and crystal building of deposits through their adsorption on the cathode surface. The widened electrochemical window, superior thermal stability, negligible or low vapor pressure and the environmentally friendly characteristics of ionic liquids (ILs) permit them to be promising replacements for traditional, toxic and volatile organic solvents.

Keywords: Electrodeposition, Ni-Co alloy, Ionic liquids, additives, Cathodic current efficiency, Voltametric measurements.

1. INTRODUCTION

Several coating processes, including evaporation, hot metal processes, painting, thermal spraying, metallizing and electrodeposition [1], are available commercially. These coating processes are used to protect surface functionality and extend the component's life. Electrodeposition or electroplating is defined as an electrochemical process in which an applied potential or current is used for deposition

of a dense, uniform, and adherent single metal or alloy film by the reduction of metallic ions onto a conductive substrate, including foils, wires and electroforms.

Electrodeposition processes have widespread uses due to their interesting properties compared to other coating methods. Electrodeposition is considered to be an economical and environmentally friendly process due to its lower operating temperature and pressure requirements, simpler instrumentation, ease of fabrication and high-quality deposits. More interesting properties include the possibility of predicting the chemical composition of deposits and easy control of deposit properties by changing the electrodeposition parameters. The most common parameters are pH, bath composition, temperature, current density, and additives. In addition, the electrodeposition process can achieve a high level of chemical tunability, free porosity and uncontrolled oxide inclusion, can easily control the film thickness, and can obtain good metal films on semiconductors and on a fabricated protein chip [1][2][3][4][5][6][7][8][9][10]. The main efficient typical properties of deposited films are the uniformity of the film thickness and dense, smooth, and bright surfaces with finer-grained structures. There are other typical properties of deposited films, including great adhesion to the substrate, high hardness, strength corrosion resistance, sufficient wear resistance, freedom from internal stress and good ductility. Moreover, electroplating baths have many important features. They are stable and have a cathodic current efficiency and throwing power, which are defined as the ability of the plating solution to produce deposits of more or less uniform thickness on irregularly shaped cathodes [2].

The electrodeposition process is performed by a specific system that contains a specialized cell. The components of an electrodeposition cell are illustrated schematically in Figure 1. The main component is an electroplating bath that contains a conducting salt and a metal source (metal to be plated in a soluble form), as well as additives and a buffer. The cell also consists of an electronically conducting cathode, (i.e., the substrate or work piece to be plated), a soluble or insoluble electronically conducting anode and a direct current source, which is usually a regulated transformer/rectifier.

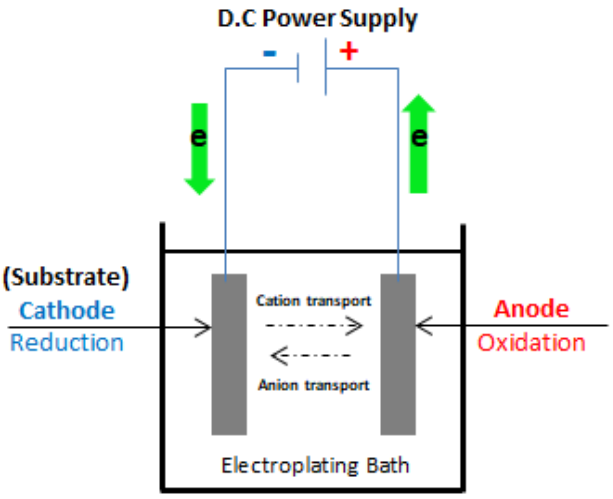

Figure 1. Component of electroplating cell.

The main important step in the electrodeposition process is cleaning or preparing the substrate surface. To obtain a strong adherence metal deposit with the desired qualities, the substrate should be free of any impurities or foreign materials, such as heavy scale oxide films, rust, workshop soils and oils, grease, dirt, and any other material. The first cleaning step is descaling, which can be done by polishing, tumbling and blasting with sand, grit or vapor, followed by a pickling process where the component is immersed in acid to remove all "foreign" matter. The other cleaning methods are buffing, alkaline soak cleaning, electrolytic cleaning and ultrasonic cleaning [1].

1.2 Electrodeposition of Alloys

An alloy is composed of two or more chemical elements, at least one of which is a metal. The alloy coating has mixed metallic properties of the parent metal. The composition of the alloy is very difficult to distinguish by the unaided eye. Through the electrodeposition process, it is possible to obtain alloy coatings from two to four metals presented in the same bath [11]. Some examples of alloy coatings are nickel–cobalt, zinc–cobalt, zinc–iron, zinc–nickel, brass (an alloy of copper and zinc), bronze (copper–tin), tin–zinc, tin–nickel, tin–cobalt, and gold–copper–cadmium. Electrodeposition of alloys has common and widespread applications in many industries, including electronics, communications, automobiles, ships, air space, machinery, gold-silver wares and jewelry, defense, toys and production of micro parts for Micro-Electro-Mechanical Systems (MEMS) and the synthesis of nanocrystalline materials [1][4][3][6][8][9][10][12][13]. Among the wide range of electroplating materials available, nickel (Ni), cobalt (Co) and Ni-Co alloys are important engineering materials used widely in numerous industrial applications.

2. APPLICATIONS OF Ni, Co and Ni-Co ALLOYS IN INDUSTRY

2.1 Applications of Nickel

Nickel and nickel alloys are considered to be important industrial materials due to their wide variety of applications (Figure 2). These applications require high corrosion resistance and heat resistance, such as aircraft gas and steam turbines, power stations, nuclear power systems, medical applications and the chemical and petrochemical industries [1][14][15][16]. Being highly resistant to tarnish and high hardness, nickel and nickel alloys have become alternatives for chromium electrodeposition in hardware, automotive, electrical and electronics accessories. Currently, Ni film is considered to be one of the most promising HER electrocatalysts among high-activity electrocatalysts due to the appropriate adsorption strength between Ni and adsorbed hydrogen (Ni-H_{ads}). Moreover, the significant Ni and its alloy coating properties include stability, high efficiency and reasonable cost of Ni and Ni alloy coatings compared with noble metals [17][18][19][20][21]. Other Ni alloy film applications are in the fabrication of anodes for Li–ion batteries [1] and protein microarray fabrication technologies [3]. Moreover, because of its favorable mechanical properties, Ni deposits are used for printing, phonography, foils, tubes, screens and many other articles [22].

2.2 Applications of Cobalt

Cobalt and cobalt alloys are considered to be important materials in engineering and are widely used in many industrial applications. This is due to their unique properties, such as good strength and thermal stability, heat conductivity, high hardness, corrosion resistance, good wear resistance, strong adhesion, optical properties, and high catalytic characteristics [23][24][25]. Moreover, Co and its alloys are used for producing nanostructure materials such as nanowires and nanotubes [4] and in various storage and magnetic devices. Moreover, Co and its alloys are applied in microsystem technology for the manufacture of sensors, actuators, micro relays, inductors and magnetic devices in the computer industry [24][26][5], as shown in Figure 2. Additionally, it is used in modern accumulators and advanced batteries, as well as in microelectronics for the semiconductor industry [4].

2.3 Applications of Ni-Co Alloy

Nickel-cobalt alloy deposits are very important due to their industrial applications (such as electronics, computers, automotive and energy storage devices, particularly in the computer field), technological (space, rocketry) applications [1][27][28], biotechnological applications [3] and powerful fabrication applications [6]. These significant applications are due to nickel-cobalt alloys having suitable magnetic, mechanical, chemical, physical and electrocatalytic properties (Figure 2). In addition, electrodeposited Ni-Co alloys are widely used as active materials for hydrogen and oxygen evolution reactions in water electrolysis, as anode materials for lithium batteries, and as catalysts for H_2O_2 decomposition [27][29]. Ni-Co films have been prepared via electrodeposition due to their low cost, easy to maintain equipment, control of film thickness, preparation of high-quality alloys, and capability of handling complex geometries. The method is environmentally friendly compared with other coating technologies, such as physical and chemical vapor deposition [1].

Figure 2. Examples of different Ni-Co coatings applied on components in various industries.

3. A BRIEF REVIEW OF NICKEL ELECTRODEPOSITION

Extensive research has shown that Ni coatings, with careful selection of the bath composition and application of appropriate techniques, provide distinguishable and adaptive solutions. Ibrahim et al. [22] investigated Ni electrodeposition on steel substrates from acidic citrate baths. The CCE% was high (91.7%), but the TP% of these baths was poor (7.4%) and strongly dependent on the operating conditions. The Ni deposit surface morphology was achieved via SEM. The results revealed that a compact, finer grained and free-porous Ni film was obtained from the optimum conditions. This superior Ni film consisted of a mixture of phases.

The effect of adding glycine as a complexing agent to the electrodeposition of Ni on copper substrates was studied [30]. The mechanism of deposition was investigated using electronic spectroscopy, potentiodynamic cathodic polarization, CV, ALSV, and chronoamperometry techniques. The Ni deposit morphology and phases were studied via XRD and SEM analyses. The results indicated an accelerating effect of glycine on Ni^{2+} reduction. Finer grains with fine microcracks and non-crystallinity of the Ni film were obtained in the presence of glycine. However, the TP%, Wagner number and corrosion resistance of the Ni deposits decreased with glycine.

The influence of Cd^{2+} during Ni electrodeposition from the acidic sulfate baths was conducted by Mohanty et al. [31]. The CCE% and the most preferred orientation (200) plane revealed from the XRD were not significantly affected in the presence of Cd^{2+} up to 500 mg dm^{-3} in the Ni electrolyte. The decrease in the exchange current density with an increasing Cd^{2+} concentration in the electrolyte confirmed the cathode polarization and inhibition effect of Cd^{+2} ions during Ni electrodeposition on both stainless steel substrates and Ni deposits. The magnitude of polarization of the cathode depends on the bath composition, which follows the order $NiSO_4+H_3BO_3$> $NiSO_4+H_3BO_3+Na_2SO_4$> $NiSO_4+Na_2SO_4$>$NiSO_4$.

The electrodeposition of Ni onto a platinum substrate from a Watts bath, including glycerol, mannitol or sorbitol in the bath as additives, was studied by Oliveira et al. [16]. The studied additives affect the kinetic parameters, as revealed via voltametric measurements, but they did not influence the deposition thermodynamically. The current efficiencies recorded high values of 95% when polyalcohols were present in the baths. At a higher hydrogen evolution state, the deposited film became clearer and brighter. This finding suggested that the formation of the dark film was prevented by the studied additives. SEM images revealed that a free-cracked Ni film was obtained from the solution, including the studied additives. Glycerol exhibited the best leveling properties.

Ibrahim [7] studied the effect of adding KNO_3 to the electrodeposition of Ni from Watt's bath. The study showed that under the optimal experimental conditions, a more leveled and stronger adherent Ni film was produced. The compositions of the optimal bath are $NiSO_4.6H_2O$ 0.63 M $NiCl_2.6H_2O$ (0.09 M), H_3BO_3 (0.3 M) and KNO_3 (0.2 M) at pH 4.6, i = 0.5 Adm^{-2}, 25°C and 10 min. The modified Watts bath has a high TP of 61%. The instantaneous nucleation of the Ni deposit was achieved from the current-time transient analysis. The XRD pattern proved that a black and pure metallic Ni film was obtained with a preferred Ni (111) orientation.

Acetone (AC) and thiourea (TU) affected the Ni electrodeposition from the ionic liquid, 1-butyl-1-methylpyrrolidinium bis(trifluoromethylsulfonyl)amide (BMPTFSA) containing Ni(TFSA)2. The

UV–vis spectra showed that the coordination surrounding the Ni(II) ions was enhanced with AC. However, the nucleation mechanism of Ni electrodeposition was not modified. The cathodic reduction potential shifted toward a more positive potential when AC was included in the bath. The addition of TU decreased the cathodic current peak with TU. The nucleation mechanism of the Ni film changed from instantaneous to progressive in the presence of TU. This result is probably due to the TU adsorption onto the electrode surface. According to the SEM, XPS and EDX characterizations, smoother Ni deposits were obtained in the presence of the two studied additives than in the absence of the additives [32].

The corrosion resistance and microhardness of Ni electrodeposited from a Watts bath has been improved via natural Kermes dye (NKD) as an effective additive using cathodic polarization behavior, anodic linear stripping voltammetry, cyclic voltammetry, cathodic current efficiency, and current-time transients. The microhardness was improved considerably, changing from 130.4 to 225 kg f mm-2 in the presence of 8.0 x 10^{-5} M NKD. Moreover, the corrosion resistance of the Ni coating was enhanced approximately five times in the presence of 1.0 x 10^{-5} M NKD. However, NKD did not change the preferential orientation of the Ni crystal planes, as shown by the XRD analysis [33].

High-quality films of the Ni-Mn alloy were prepared in a choline chloride–urea ionic liquid containing both 0.20 M $NiCl_2 \cdot 6H_2O$ and 1.50 M $MnCl_2 \cdot 4H_2O$ with the addition of glycine in order to control the composition, microstructure and properties of the film. The effects of the glycine concentration and current density on the electrodeposition mechanism of Ni–Mn alloy films were studied by CVs. The reduction of Ni^{2+} ions was inhibited in the presence of glycine. However, the reduction of Mn^{2+} is promoted by glycine. The Mn content in the Ni–Mn alloy increased when the concentration of glycine and current density were increased. The lowest corrosion current of 3×10^{-7} A/cm^2 was exhibited in the Ni–Mn film with 3.1 % Mn compared with the other prepared films. The Ni–Mn film with 3.1 % Mn exhibited a higher corrosion resistance than the pure Ni film in a 3.5 wt.% NaCl solution [34].

The Zn-Ni-Fe coating was co-deposited in the absence and presence of ascorbic acid (AA) and the Fe2+ in solution on a low carbon steel substrate. The Fe2+ ions showed an insignificant influence on the electrodeposition process, as illustrated in the CVs. However, a significant influence occurred after spontaneous oxidation of Fe2+ to Fe3+ and the consequent formation of Fe(OH)3. The increase in the Fe(OH)3 in solution led to a greater inhibition of the electrodeposit by adsorption at the cathode and blocking the active sites that would be occupied by the metal ions. In general, the pure Zn in the Zn-Ni-Fe co-deposit was decreased by the hydroxide and obtained a more compact and smooth coating of Zn-Ni-Fe compared to Zn-Ni. However, the Zn content in the deposit increased in the presence of AA because of the increasing overpotential deposition by complex adsorption on the surface of the cathode. In conclusion, the Zn-Ni and Zn-Ni-Fe coatings deposited from AA included in solution were more compact and had more uniform coatings than the other coatings obtained from the free AA solution. This enhancement in the coating was due to an increase in the grain nucleation rate as a result of the increase in the overpotential in the presence of additive [35].

Ni-P thin films were obtained in the presence of various additives (saccharine, glycine, pyridinium propyl sulfonate, coumarin, sodium citrate, and cerium sulfate). The results showed that at the appropriate concentration of each studied additive, except saccharine, a noticeable improvement in the corrosion resistance, especially at high potentials (an approximately 25% increase in the instantaneous corrosion efficiency and an approximately 300% corrosion efficiency at high potentials)

decreased the surface roughness (by approximately 10 to 55%) of the Ni-P thin films. Thinner, more compact, and non-porous deposits were obtained from the system including additives. All the additives, except saccharine, increased the P content in the Ni-P films, which thus maintained their amorphous structure; saccharine highly suppressed the incorporation of P inside the Ni lattice, and a mixed amorphous-crystalline structure was stabilized [36].

The synergistic effect of vanillin, sodium lauryl sulfate and gelatin as additives on Re-Ni electrodeposition on copper substrates from aqueous solutions has been studied [37]. The effects of additives and many other factors, such as bath composition, operating conditions, and current densities, were investigated to improve the surface morphology of Re-rich Re-Ni alloy deposits. The presence of additives exhibited a significant influence on the composition, surface morphology and cracking pattern of the deposit. In addition, the surface morphology of the Re-Ni alloy changed from a uniform and smooth surface without additives to a relatively coarse-grained surface with additives. The non-favored cracked coating was enhanced in the presence of additives in the optimal bath containing 34 mM ReO_4^-, 124 mM Ni^{2+} and 343 mM $[citrate]^{3-}$. At lower Ni ion concentrations (30–50 mM) in the presence of additives, almost pure Re films were formed. Amorphous behavior was exhibited in the Re-rich alloy.

4. A BRIEF REVIEW OF COBALT ELECTRODEPOSITION

Various studies have illustrated the specific conditions and bath compositions in detail, including additives in the electroplating of Co onto various substrates:

Abd El Rehim et al. [14] investigated Co electrodeposition onto steel substrates from acidic sulfate solutions containing sodium gluconate. The cathodic current efficiency was high (~95%) and depended on the operating conditions. The surface morphology indicated that the as-deposited Co under the optimum conditions is composed of compact, microcracked, fine grains covering the entire substrate surface. The microhardness of the as-deposited Co from the present bath is generally high. The TP of the present bath was low (≈ 5.9 %).

Highly adherent, lustrous grey Co film was successfully electrodeposited from an acidic glycine complexing bath on copper substrates. Voltametric measurements, including potentiodynamic cathodic polarization, CV, ALSV and chronoamperometry, were studied. The cathodic potential shifted toward a more negative direction when glycine was included in the bath. This finding indicated that glycine complexes with Co ions act as inhibitors. Glycine-containing baths obtained deposits with a higher TP and higher hardness than those deposited from glycine-free baths. The SEM images revealed that finer grains with tiny microcrack Co deposits were produced from glycine-containing baths. Co coating are non-crystalline, and the degree of non-crystallinity grows with an increasing glycine concentration [23].

In situ SERS measurements were studied for electrodeposition and stripping of Co films on Au substrates from a coumarin-containing bath. Both cathodic deposition and anodic stripping were investigated under suitable conditions. Many electrochemical polarization types have been considered, such as cathodic potential staircases, potentiostatic electrodeposition and potentiostatic stripping of potentiostatically pre-electrodeposited Co layers. Potential-dependent spectra measured via SERS enhancement identified bands that allowed spectral assignment of coumarin and its reduction and

hydrolysis products. Moreover, the surface enhancement degree typically increased with the electrodeposition time. The spectral patterns depend on the electrodeposition potential and the plating time. The great spectral quality and remarkable sensitivity to the mode of grown Co film were investigated from the stripping analysis [38].

The effects of coumarin and thiourea (TU) as addition agents on the electrodeposition of Co were investigated in an amide-type ionic liquid, 1-butyl-1-methylpyrrolidinium bis(trifluoromethylsulfonyl)amide (BMPTFSA). In both additive cases, the deposition potential of Co shifted toward a less negative direction. The surface morphologies of the deposits were improved to be more uniform, with finer grains and greater adhesion deposits. This finding was due to the specific adsorption of both additives on the cathode surface. On the other hand, there was no change in the coordination environment of Co^{2+} in the presence of coumarin. In contrast, in the case of TU, the dissolved Co species were changed from $[Co(TFSA)_3]^-$ to $[Co(TU)_4]^{2+}$. The deposition potential of Co from $[Co(TU)_4]^{2+}$ was more positive than that of $[Co(TFSA)_3]^-$, and the surface morphology of the deposit obtained from $[Co(TU)_4]^{2+}$ exhibited a higher enhancement [15].

Santos et al.,[5] investigated cobalt electrodeposition from sulfate solutions containing boric acid by using EQCM coupled with potentiostatic techniques and the current–time transient. The Co electrodeposition mechanism was affected significantly when the bath temperature increased. At 25°C, only direct Co reduction is observed, while at 48°C, $Co(OH)_2$ can be observed from the calculated apparent M/z values. These results suggest that $Co(OH)_2$ can be formed simultaneously with Co deposits and that the buffer contribution of boric acid was ineffective at 48°C. For high temperatures the adsorption mechanism was greater. This leads to an increase in the active surface area available for HER, and $Co(OH)_2$ can be formed.

Manhabosco et al. [26] studied the influence of saccharin as an additive in the electrodeposition of Co thin films on silicon. Co reduction, kinetics, and hydrogen evolution were affected via the saccharin molecules and a complexation process. The additive improves the appearance and brightness of the metallic films. The brightness increases as the additive concentration rises.

Barrera et al.[25] highlighted the effect of KNO_3 as an additive in Co electrodeposition from an aqueous solution onto a stainless steel substrate. The composition of the bath was 1.17 M Co(II), 0.98 M H_2SO_4, 0.56 M KC1, and 0.2 M H_3BO_3. Analysis of the deposited Co surface via AFM and SEM analysis revealed that the black Co film was more dispersed and had a higher roughness than the white Co, while the white Co electrodeposition mechanism was shown to occur via multiple 3D, and nucleation was limited by lattice incorporation of Co atoms into the growth centers.

Co-Pt thin films with many thicknesses were obtained by electrodeposition from an aqueous hexachloroplatinate solution under controlled conditions (saccharin as an additive, pH 5.5, controlled potential) on a sputtered Ru-substrate. The XRD measurements revealed that Co-Pt films crystallize in the hcp phase. The compositional analysis of the films showed a “composition gradient”, which indicated that the film thickness increased with and increasing Co concentration until reaching a steady value (for thicknesses > 110 nm). MFM measurements were used to analyze the structure and width of the magnetic domains. The results indicated that the thickness was dependent in the range of 20-250 nm [4].

5. A BRIEF REVIEW OF NICKLE-COBALT ALLOY ELECTRODEPOSITION

Electrodeposition of Ni-Co alloy and details of the co-deposition mechanism process, including specific conditions, were investigated in the following studies:

A modified Watt's bath was used in [24] to produce new Ni–Co alloys with various Co contents via electrodeposition. The Ni–Co alloy electrodeposition mechanism and its surface morphology were investigated via EIS, SEM and XRD. The results showed that with an increasing Co^{2+} ion concentration in the electroplating bath, the charge transfer resistance increases, and the Warburg impedance of growth in the Ni−Co layer decreases. The Co content in the Ni−Co alloy coatings increased anomalously, and the strong Ni-Co (111) texture improved progressively. In addition, as the Co content increased up to 45% in the alloy coating, the grain size decreased and the hardness and strength of the alloy consequently increased. However, at 55% Co, such parameters decreased.

The Ni-Co-W alloys were produced by electrodeposition on an Al net substrate in the absence and presence of sodium citrate. The composition of the electrolytic baths was 20 g/L Ni, 8 g/L Co, W in the range 2-8 g/L and boric acid at 20 g/L. The temperature of the bath and current density values were changed in the ranges of 30-60°C and 260-350 $A/m^{2,}$ respectively. The best current efficiency and specific energy consumption results were obtained in the presence of sodium citrate in the range of 30-60°C, while the cell voltage was lower. The morphology and structure of deposits were investigated to obtain the best deposit. The XRD affirmed that the main difference in the pattern of samples was from sodium citrate. The electrolyte containing sodium citrate also exhibited an Ni fcc structure formation [39].

Ni-Co-Fe-P quaternary alloys were prepared via electrodeposition. By changing the H_3PO_3 concentration in the plating electrolyte, the P content in the alloy was controlled**.** Consequently, the P content of the Ni-Co-Fe-P coating increased with an increasing H_3PO_3 concentration in the electrolyte. This increase in the H_3PO_3 concentration enhanced the coating morphology and led to the production of a refined grain size, a pure amorphous material. The microhardness of the quaternary alloy coating grew rapidly by approximately two times. The achievement of the anodic polarization results revealed that the corrosion resistance of the alloy coatings decreased at lower H_3PO_3 concentrations but then increased at higher H_3PO_3 additions. The best erosion–corrosion resistance was obtained with the Ni-Co-Fe-12.92P coating. This finding is in good agreement with the hardness and the corrosion current density [11].

Ni-Co-Sn alloys were obtained by electrodeposition from a chlorine chloride (ChCl)-ethylene glycol (EG) deep eutectic solvent (DES). Both the Ni-Sn and Co-Sn alloys were electrodeposited. The Sn^{2+} ions supported DES electrochemical stability. CV measurements confirmed the alloy formation because there were no cathodic or anodic peaks for individual elements. An XRD analysis revealed that the binary and ternary alloy of Ni exhibited only the Ni lattice, and the other elements were included in the Ni lattice. Furthermore, this result was confirmed via SEM images, and binary and ternary alloys of Ni exhibit similar morphologies. The potentiodynamic polarization analysis revealed that the ternary Ni-Co-Sn alloy coating has the highest stability in the anodic region in an alkaline solution [40].

The influence of nano-Al_2O_3 particles has been studied in Ni-Co deposit films. The presence of such particles improved the corrosion protection, the surface morphology, and the structure of Ni-Co alloy layers compared to free-Al_2O_3-Ni–Co deposited alloy, as exhibited in the potentiodynamic

polarization results and SEM. Moreover, the resistance against corrosion of the alloy was further improved as the pH of the electrodeposition bath and the Co content in the alloy increased. More homogeneous, fine-grained deposits were obtained by increasing the Ni^{2+}/Co^{2+} ratio in the electrolyte [28].

Yang et al. [41] produced bright Ni-Co alloy foils on a titanium substrate via electrodeposition from an acid chloride-sulfate bath by optimization of the electrodeposition parameters. The bright deposit current density, temperature, and pH value range are 3-4 A dm^{-2}, 40-50°C and 2-3, respectively. The optimized concentration of cobalt sulfate is 20 g/L and that of saccharin is 2-3 g/L. The crystallographic structure of Ni-Co deposited foil is the fcc Ni solid solution. The deposit is uniform fine grained and shows a good toughness and low residual stress.

6. CIRCUIT FOR ELECTRODEPOSITION.

The plating cell, as shown in Figure 3, is made from transparent Perspex in the form of a rectangular trough. The cell has inside dimensions of an 11 cm length, a 3 cm width and a 2.5 cm height, and will be used for measurements of cathodic current efficiency and all other voltametric measurements. For the throwing power and throwing index measurements, the Harring Blum cell shown in Figure 6, which has inside dimensions of a 17.5 cm length, a 3 cm width and a 2.5 cm height, is used. Both cells are designed with vertical grooves on each of the walls side that are 2.5 cm apart from each other, and the electrodes could be placed vertical at fixed distances in the cell. Table 1 summarizes the electrodes employed in the electrodeposition process according to different techniques reported in [7][14][22][23][30][33][42][43][44][45][46].

Table 1. Summary of electrodes used for different techniques.

Electrodes		Technique
Anode	Pt sheet	CCE % TP %
Cathode	Cu or steel sheet	CCE %
Two parallel cathodes	Cu or steel sheet	TP %
WE	GCE	CV, ALSV and chronoamperometry.
	Cu sheet or steel sheet	Potentiodynamic cathodic polarization.
	Metal or alloy deposits	Corrosion resistance (EIS, potentiodynamic polarization)
CE RE	Pt sheet SCE	CV, ALSV, chronoamperometry, potentiodynamic cathodic polarization and corrosion resistance

The electric circuit shown diagrammatically in Figure 3,a was used for electrodeposition and CCE% measurement. It consists of an electroplating cell in which the copper [23][30][44][46] or steel

[7][14][22][33][42][43][45] cathode is inserted with a platinum anode and fixed in their appropriate positions. A D.C. regulated power supply is connected to supply the required current density. Figure 3,b shows a diagram of the electric circuit used for potentiodynamic cathodic polarization [22][42][43][44][45] and corrosion resistance [23][30][33][46] measurements. The electroplating cell consists of an appropriate WE inserted with the platinum sheet as a CE (Table 1). In the corrosion resistance measurements, the WE was metal or alloy deposits. The CV, ALSV and chronoamperometry (potentiostatic current-time transients) [23][30][43][44][45][46] were measured by an electrical circuit, as shown in Figure 3,c. This consisted of an electroplating cell, in which a platinum sheet is used as a CE, the GCE is used as the working electrode (WE) and the SCE is used as the reference electrode (RE), Table 1. The SCE as an RE is placed near the working electrode, and the three electrodes are connected to a potentiostat/galvanostat, which is connected to a personal computer. Software packages were used to measure and analyze data. The throwing power and throwing index of the plating solutions are measured in a Harring Blum cell [14][22][23][30][33][42][43][44][45][46], as shown in Figure 3,d, which has inside dimensions of a 17.5 cm length, a 3 cm width and a 2.5 cm height is used. The cell is provided with one platinum anode between two parallel copper or steel sheets as cathodes (Table 1) at different distances (1:1-1:5).

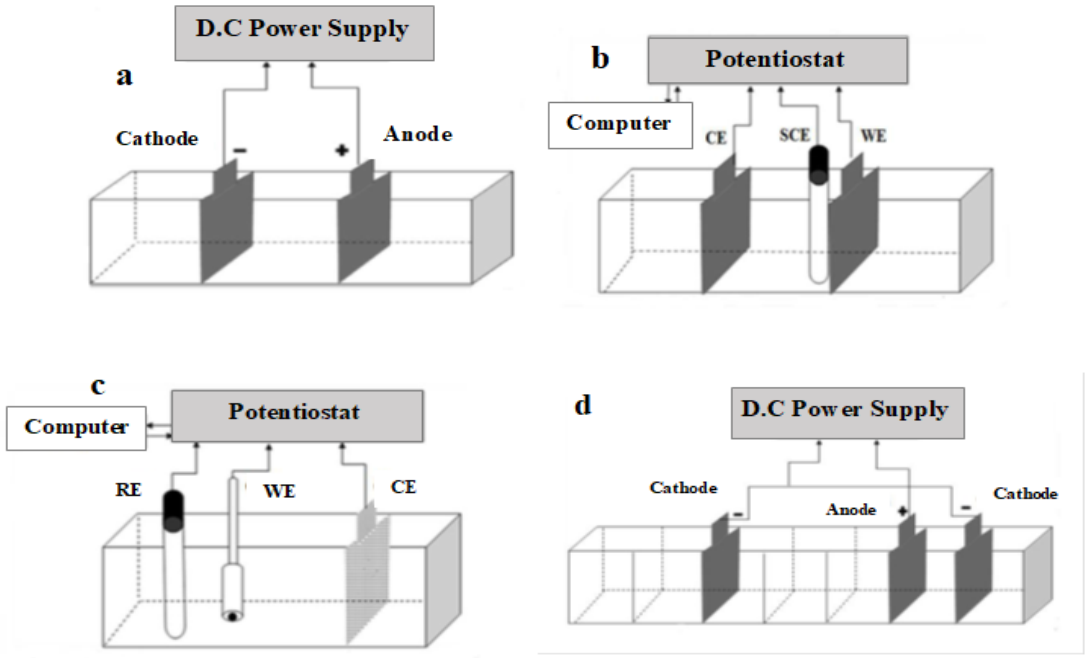

Figure 3. The electroplating cell and the electrical circuit used for measuring (a) the electrodeposition and CCE%, (b) potentiodynamic CP and corrosion resistance, (c) CV and ALSV, and (d) the throwing power and throwing index.

For individual deposition of the single metals, the CCE% is simply calculated according to Faraday's law from equation (1):

$$\text{CCE } \% = \frac{Wp}{Wt} \times 100 \qquad (1)$$

Where W_p is the practical weight of the deposit, and the theoretical weight of the deposit W_t is calculated using Faraday's law [47][2]. The CCE% of the alloys is determined by the method reported in [1][47]. The partial current efficiencies % of the parent metals, CCE_{Ni} % and $CCE_{Co,}$ in the alloy were calculated using the following relations:

$$CCE_{Ni}\ \% = \frac{W_{Ni}}{Wt} \times 100 \quad (2)$$

$$CCE_{Co}\ \% = \frac{W_{Co}}{Wt} \times 100 \quad (3)$$

Where w_{Ni} and w_{Co} are the practical weights of the Ni and Co deposits, respectively. The W_p of the parent metals in an alloy are obtained from the composition of the alloy. The alloy composition is then determined by an EDS analysis. Then, the total alloy efficiency, CCE_{alloy}, is equal to the sum of CCE_{Ni} and CCE_{Co}:

$$CCE_{alloy} = CCE_{Ni} + CCE_{Co} \quad (4)$$

Through power (TP) and throwing index (TI) calculations, the two cathodes (Cu) are weighed before and after electrodeposition for a certain time at a settled current density. In each case, the throwing power is calculated at the linear ratio "L = 3" using Field's formula [1][2].

$$TP\ \% = \frac{L-M}{L+M-2} \times 100 \quad (5)$$

Where L is the linear distance ratio and M is the metal distribution ratio. These are defined as reported in [1][2]

$$\text{Linear ratio (L)} = \frac{\text{Distance of a far cathode}}{\text{Distance of a near cathode}} \quad (6)$$

$$\text{Metal ratio (M)} = \frac{\text{Weight of deposit on near cathode}}{\text{Weight of deposit on far cathode}} \quad (7)$$

With regard to the above formula, the TP of different solutions can be obtained. From the experimental weights of the metal deposited on the two cathodes, the near and far cathodes, the metal distribution ratio (M) is calculated and then plotted versus the linear ratio (L) on arithmetic coordinates. The reciprocal of the slope of this plot is called the "throwing index".

7. IONIC LIQUIDS (ILs)

The molten salts ,which are melted at lower than 100 °C and contained of cations as well as anions, are classified in the chemistry as ionic liquids. The unstable charge positions of the ionic liquid ions cause them to melt at a low temperature [48]. Commonly used ionic liquids cations are those consisting from alkylpyridinium, alkylimidazolium, alkylphosphonium, alkylammonium and alkylguanidinium. However, the most common ionic liquids anions are chloride, tetrafluoroborate and methylsulfate. Generally speaking, the various ionic liquids anions control the miscibility points of these compounds in water. Moreover, the obtaining of ILs is commonly achieved by metathesis, beginning from pioneer chloride salts. The ILs cations are adsorbed at the surface of cathode at the appropriated deposition potential. Consequently, the fabric of the double layer is depended on cation, which impacts some ILs such as conductivity and viscosity of these solutions [49]. The ionic liquids are considered as versatile properties compounds which are consisted from several kinds including binary and ternary mixtures. The most common ionic liquids are classified into three main systems as the following:

a) Systems established from $AlCl_3$ and organic salts such as 1-butylpyrridinium chloride and 1-alkyl-3-methylimidazolium chloride.

b) Systems established from organic cations as in the first group as well as anions BF_4, PF_6 and SbF_6.

c) Systems established from the aforementioned organic cations with anions of the type CF_3SO_3 and similar [9].

7.1 Properties and Advantages of Ionic Liquids:

The unique structural characteristics of ionic liquids give them several distinct characters which qualified them for various applications. The most important ionic liquid property is its large electrochemical window (> 5 V). This property gives access to electrodeposits of some elements, such as Mg, Al, Ta and Ti, that are hard to electrodeposit from aqueous or organic media at modest temperatures. The electrodeposition process is affected via both anions and cations of ILs. Generally, the physical characters of the IL salt, such as its crystal structure and the appearance of its surface morphology, are controlled by cations. However, the main role of the anion is exhibited in the chemical reactivity of ILs and its stability. Furthermore, the anions performed an effective role in the coordination geometry as well as other factors such as the nucleation mechanism, the potential and the current of metal reduction. Moreover, a convenient choice of both cation and anion radicals influences the ILs solubility, polarity, viscosity, and density. Moreover, a higher ILs conductivity, in the range from 10^{-3} to 10^{-2} Ω^{-1} cm^{-1}, in the comparison with that of organic solvents or electrolytes qualifies ILs for performing the electrodeposition process at low temperatures. The ILs effort an ability for performing some experiments which required very high temperatures, up to 400 ℃ due to its extremely low vapor pressures, in the range from 10^{-11} to 10^{-10} at room temperature.

The high thermal stability of ionic liquids has qualified them for use at wide range of temperature. In the environmental perspective view, ionic liquids are considered as more environmentally friendly, greener and cleaner than many toxic solutions. Finally, ionic liquids became more effective solvents in the both organics and inorganics medias. The electrodeposition potentials of the single metal ions are much closer together in ionic liquids, enabling easier electroplated alloys [47][50]. In conclusion, ILs are considered as definitely advanced promising technological solvents which are designed for a convenient and particular applications.

7.2 Applications of Ionic Liquids in Electrodeposition:

The unique, convenient and promising characters of ionic liquids, several industries applied ILs at many important aspects. The most interesting application could be mentioned in brief including synthesis, electrodeposition, extraction processes, electrochemistry, photochemistry, liquid crystals, CO_2 capture, green corrosion inhibitors for metal anti-corrosion, desulfurization of fuel, enzymatic synthesis, lubrication, rocket propulsion and thermal storage devices. In the electrochemistry:

- The very modest vapor pressure of ionic liquids led them for green using in the open galvanic solutions at variable temperatures via preventing the emission of the deleterious vapors. As result, the amount of volatile organic compounds released into the atmosphere reduced significantly.

- A significant energy savings are afforded through the ionic liquids great conductivity compared with aqueous solutions.

- The ionic liquids provides green, recyclable and environmentally friendly options for synthetic organic chemistry, separation sciences, chemical and engineering sciences.

- The ionic liquids, due to their high ion concentration, excellent stability and great ionic conductivity, become a beneficial materials for electrical energy storage devices, such as electrolytic capacitors, batteries and fuel cells, as well as supporting media for catalysts [50].

7.3 The Importance of Ionic Liquids as Additives and Corrosion Inhibitors.

In the electrodeposition of metals and alloys, additives are commonly used due to their convenient roles. The additives have influenced in both the coating films characterization and the microstructure of deposits crystals. This phenomenon occurred through additives adsorbtion on the electrode surface. Some traditional colloidal and organic compounds additives have been widely used in industry and have achieved strong additives. However, many organic additives are easy and fast to degrade or they are not green materials. Moreover, many organic substances have some disadvantages, such as a low thermal stability, a poor chemical activity and high toxicity. Consequently, there are continuing efforts for obtaining more efficient additives that combine a good stability, high efficiency and environmental friendliness.

There is a similarity between additives of electrodeposition and corrosion inhibitors in terms of their mechanism effect, which is both of their adsorption abilities on the substrate surface. However, many commercially common inhibitors are toxic substances that should be replaced by new, more eco-friendly ones. Currently, many researchers have focused on using inexpensive, efficient molecules and environmentally friendly materials as corrosion inhibitors [51]. The main difference between them is that the additives are studied under an electric field. The adsorption behavior are controlled by the electric field distribution. In contrast, there is no galvanization in the corrosion inhibition process. The adsorption of corrosion inhibitors depends on certain physicochemical properties of the inhibitor group, such as electron density at the donor atom, the π-orbital character and the electronic structure of the molecule [51].

ILs are compounds that are contained from two main radicals, organic cations and organic or inorganic anions in the liquid state at low temperatures. The high cationic configuration of ILs readily facilities them for adsorption on the cathode surface under an electric field. Moreover, some functional groups, such as the –C=N– group, –C=O, I^-, F^-, and electronegative heteroatom in the molecule of ILs enable them for a spontaneous adsorption on the metal substrate surface. This finding is due to the specific interaction between the active centers of the functional groups in the ILs molecules and the metal surface [51]. Interestingly, ILs have become a promising alternative for non-environmentally volatile organic compounds.

7.4 Ionic Liquid as an Electrolyte Or Additive In Electrodeposition.

Studies have proven the striking function of ionic liquids as electrolytes or additives in the electroplating of alloys:

Zhu et al. [27] mentioned Ni electrodeposition from an ionic liquid, 1-butyl-1-methylpyrrolidinium bis(trifluoromethylsulfonyl)amide (BMPTFSA) containing $Ni(TFSA)_2$, by using acetonitrile (ACN) as an addition agent. ACN exhibited a change in the BMPTFSA ionic liquid color as a result of changing the Ni(II) coordination number from $[Ni(TFSA)_3]^-$to $[Ni(ACN)_6]^{2+}$, as confirmed by UV–vis and FT-IR spectroscopy. The Ni coating nucleation mechanism remained constant even though the Ni ion coordination environment was changed. However, a higher range of nuclei is generated on the cathode surface, as confirmed via chronoamperometric measurements. The SEM images showed that smoother Ni deposits were obtained from Ni(TFSA)2/BMPTFSA with ACN.

The same authors of a previous study discussed the effective role of coumarin and saccharin [52] as additives in Ni electrodeposition under the same ionic liquid solution. As confirmed via UV-vis analysis, the Ni^{2+} coordination number stayed the same as coumarin or saccharin. However, the overpotentials for the Ni^{2+} reduction increased, but the current density decreased. The diffusion coefficients of Ni^{2+} with both studied additives were estimated to be near those in the free-additive electrolyte, as confirmed by a chronoamperometry study. The nucleation mechanism model of the Ni coating fluctuated from instantaneous to progressive with both coumarin and saccharin. The influence of the two studied additives exhibited a good enhancement on the Ni deposit surface morphology.

The electrodeposition mechanism of Ni–Cu alloy coatings was obtained from a choline chloride–urea (1:2 molar ratio) eutectic-based ionic liquid (1:2ChCl–urea IL) on a Cu substrate. Cyclic voltammograms confirmed the high possibility of obtaining Ni–Cu alloy films from a 1:2 ChCl–urea ionic liquid bath with no need for complexing agents due to their close onset reduction potentials. The nucleation mechanism of Ni–Cu deposits followed the instantaneous 3D model, as revealed via chronoamperometric analysis. A denser surface of the Ni–Cu alloy coating was produced at a lower deposition current density and a lower Cu content in the alloy, as revealed by the SEM/EDX analysis. Under similar conditions, the XRD pattern showed an enhancement in the preferential orientation of the Ni(1 1 1) plane with a high current density. The greatest corrosion resistance of the Ni–Cu alloy coating was obtained with ~17.6 % Cu content in the alloy, as confirmed via potentiodynamic polarization [53].

The presence of many ionic liquids in the electrolyte containing five transition metals was obtained by dissolving bistriflimide salts of Ag, Cu, Co, Ni and zinc in 1-butyl-3-methylimidazolium bistriflimide ([bmim][Tf2N]) in a 1:2 molar ratio. With the exception of the Ni system, for all ionic liquids it became possible to obtain the metal deposits in a normal air atmosphere. Therefore, a homogeneous and free-cracked silver deposit was obtained potentiostatically from the studied ionic liquid.

Silver deposits are considered electroactive and follow a progressive nucleation mechanism in non-wet media. In contrast, the other systems, including the copper-cobalt and zinc-bearing systems, were strongly moisture sensitive. The copper electrodeposits could only be obtained from wet media. The nucleation and growth mechanism obey the progressive model. Consequently, globular crystal blocks are formed. Silvery zinc coatings with strong adherence could be achieved in both “wet” and

"dry" media. In conclusion, in all previous cases, except for Ni, both metal or mixed metal oxides can be electrodeposited via direct electrodeposition at room temperature in open air conditions [54].

Ni-Mo and Co-Mo alloy coatings were electrodeposited from Ch-Cl-based ionic liquids onto Cu substrates. The electrolytes contained Ni^{2+}, Co^{2+} and Mo^{6+} ions in Ch-Cl-urea-citric acid. Ni-Mo alloys with 2–35 Mo% and Co-Mo alloy with 6–63 Mo% exhibited excellent adherence and uniformity and a nanocrystalline structure, where the average crystallite sizes=3-7 nm. Moreover, Ni-Mo alloy, with 8–9 Mo%, and Co-Mo alloy, with 10–12 Mo%, appeared to have greater corrosion protection than those electrodeposited in classical aqueous electrolytes, suggesting the gradual formation of a protective passive film on the surface [55].

Thick Ni-Fe-Mo and Ni-Fe-W alloy films were electrodeposited using a constant current technique on a Cu microwire (50 μm) from a citrate bath, including a 1-dodecyl-3-methylimidazolium chloride IL. The magnetic properties, composition and structure of the coatings were investigated in the presence of IL. Uniform, free damage and the amorphous/nanocrystalline coating were obtained under optimized experimental conditions as shown from SEM and XRD analysis. EDX measurements revealed that the coatings with $Ni_{32}Fe_{48}Mo_{20}$ and $Ni_{52}Fe_{33}W_{15}$ exhibited the best properties. The relatively high saturation magnetization (65.3 and 37.08 emu/g), low coercivity Hc (4.0 and 12.0) and satisfactory GMI ratios (102.2% and 20.1%) qualified this coating as a promising material for magnetic sensor applications. The content of both W and Mo could be easily tuned in a solution containing IL. The studied IL played a very effective role in producing compact and uniform alloy coatings. These films of desired composition are considered to be prospective films for use as catalysts and electrode materials in different industries, such as fuel cells, hydrogen revolution reactions or sensing elements in magnetic sensors [56].

Ni–Mo alloy coating was deposited from an ammonia citrate bath including 1-ethyl-3-methyl-imidazolium chloride ionic liquid as an additive on mild steel by using the pulse plating technique. The results showed that the Mo content in the Ni–Mo alloy increased to more than 50 % under the optimal conditions of 10 ppm ionic liquid, pH 8.5, and 200 rpm rotation. Moreover, an adherent, compact and bright Ni–Mo alloy coating was obtained under the optimal conditions, as revealed from the SEM images. The XRD patterns showed amorphous/nanocrystalline Ni–Mo coatings deposited under pest conditions [57].

In his major study, Ibrahim et al. identified the role of a 1-butyl-3-methylpyridinium bromide [BMPy]Br ionic liquid as an additive on zinc coating characteristics from acidic sulfate electrolytes. Cathodic polarization and cyclic voltammetry measurements were employed to determine the deposition mechanism. A high nucleation overpotential was shown in CVs in the presence of [BMPy]Br, confirming the inhibition of Zn ion deposition. The kinetic parameters were calculated from the Tafel plots and exhibited a strong inhibiting effect of [BMPy]Br on Zn ion reduction. A homogenous and finer-grained Zn coating was obtained at low [BMPy]Br concentrations. The XRD pattern showed that the studied additive had no effect on the Zn coating crystal structure, but strongly affected the crystallographic orientation of the crystal planes. The TP of the deposition electrolyte with [BMPy]Br was more than doubly increased [42].

8. CONCLUSION

Electrodeposition is considered to be an economical and environmentally friendly process due to its interesting properties. Nickel and its alloys are used for an enormous variety of industrial applications, especially those that require high corrosion, heat resistance and hardness. Currently, metallic Ni is considered to be one of the most promising HER electrocatalysts. Cobalt and its alloys are considered interesting materials in the engineering field, which qualifies them for common utilization in many industrial applications due to their unique properties, including great corrosion protection, high strength and hardness, good adhesion, thermal stability, heat conduction, desirable optical properties, and excellent catalytic characteristics. The novel, green and efficient addition agents in Ni and Co and their alloy electrodeposition process have become attractive goals for many researchers. Many attempts have been made to find new additives to improve deposit characterizations and operating conditions. These attempts are mainly represented in the CE as well as cathodic polarization. Many researchers have successfully achieved a convenient correlation among the deposit morphology, crystallographic orientations of grains, CCE% values of the electrolytes and the reflected kinetic parameters. The following summaries conclude the main important key points:

- In Ni electroreduction, acidic citrate and polyalcohol additives in the electroplating baths exhibited high CCE% (91.7% and 95%, respectively), and the Ni deposit was composed of free-porous, finer grains and compact covering. Adding KNO_3 to Watt's bath produces smooth and highly adherent black Ni with a high TP of 61%. Glycine played an accelerator role in Ni^{2+} electroreduction. The SEM and XRD analysis revealed finer grains with fine microcracks and an increasing non-crystallinity of the Ni film. Glycerol, mannitol or sorbitol showed excellent leveling properties because the smoothest film was obtained. The corrosion resistance and microhardness of the Ni deposited from a Watts bath have been improved by natural Kermes dye (NKD) as an efficient additive.

- In the Co electrodeposition, solutions containing the CCE% (~95%) and the microhardness of the Co deposit were high in the presence of sodium gluconate. Glycine acts as an inhibitor and obtained a higher TP and hardness than glycine-free baths, and the non-crystalline degree of the Co coating grew with an increasing glycine concentration. The surface morphology of the Co coating with sodium gluconate and glycine had compact, fine grains with the appearance of fine microcracks. In both the coumarin and thiourea additives, the deposition potential of Co shifted toward a more positive direction. The surface morphology of the deposits was enhanced to a more homogenous, lower granular and stronger adhesion. This finding suggests the specific adsorption of both additives on the cathode surface. Boric acid and the EQCM technique increase the adsorption rate and the active centers available for HER in Co electrodeposition. As a result, $Co(OH)_2$ can be obtained at high temperatures. Adding saccharin modifies the metallic appearance of the Co film, which shows a higher brightness as the additive concentration increases.

- In the co-deposition of Ni–Co alloys, as the Co content increased above 45% in the alloy deposits, the grain size became finer, but the hardness of the alloy consequently increased. To obtain the Ni-Co-W alloys, the best CCE% and specific energy consumption results were obtained with sodium citrate. The refined grain size, pure amorphous material, microhardness and corrosion resistance of the Ni-Co-Fe-P quaternary alloy deposit increased significantly at high H_3PO_3 concentrations in the

electrolyte. The Ni-Co-Sn alloy electrodeposited from the ChCl-ethylene glycol-DES is more stable in the anodic region in the alkaline solution, and the stability of the DES increased in the presence of Sn^{+2} ions. The presence of nano-Al_2O_3 particles improved the corrosion properties, morphology, and microstructure of the Ni–Co alloy deposit film. The Ni-Co alloy foil deposit was bright, uniform, fine grained, and had a good toughness and low residual stress with 2-3 g/L of saccharin.

The promising properties of ionic liquids (ILs) qualify them as green alternatives for volatile and toxic organic solutions. ILs contain organic cations and organic or inorganic anions that are in the liquid state, even though the temperature is low. The great configuration of their cationic and some functional groups readily led them to spontaneous adsorption on the metal surface due to the specific interaction between these functional groups and the metal surface. Many studies have proven the effective function of ionic liquids as electrolytes or additives in the electroplating of alloys as follows: more leveled deposits were obtained in Ni(TFSA)2/BMPTFSA ionic liquids with CAN. Ni–Cu alloy films from a ChCl–urea -DES ionic liquid containing ~17.6% Cu obtained the strongest corrosion resistance as a result of the dense and free-cracked structure. Good adherence, uniformity and an improved corrosion performance of Ni-Mo and Co-Mo alloy films from the ChCl ionic liquids were investigated, and both alloy films exhibited a nanocrystalline structure. A strong adherent, as well as a more compact and brighter Ni–Mo alloy was obtained from a bath including 1-ethyl-3-methyl-imidazolium chloride ionic liquid as an additive in an ammonia citrate media using the pulse plating technique. Bright and adherent thick films of Ni-Fe-Mo and Ni-Fe-W alloys were electrodeposited by a constant current technique from a citrate-based bath containing a 1-dodecyl-3-methylimidazolium chloride ionic liquid.

References

1. R.M. Al Raddadi, Cathodic codeposition of nickel-cobalt alloy coatings from acidic glycine complex baths, (2014) Taibah university, KSA.
2. E.M.A. Omar, Effect of Organic Additives on Zinc Electrodeposition from Acidic Sulfate Bath, (2012) Taibah University, KSA.
3. Y.J. Chang, S.Z. Chen and C.Y. Ho, *Colloids Surf., B.,* 128 (2015) 55.
4. O. Dragos-Pinzaru, A. Ghemes, H. Chiriac, N. Lupu, M. Grigoras, S. Riemer and I. Tabakovic, *J. Alloys Compd.,* 718 (2017) 319.
5. J.S. Santos, R. Matos, F. Trivinho-Strixino and E.C. Pereira, *Electrochim. Acta,* 53 (2007) 644.
6. C.D. Grill, J.P. Kollender and A.W. Hassel, *Phys. Status Solidi,.* 212 (2015) 1216.
7. M.A.M. Ibrahim, *J. Appl. Electrochem.,* 36 (2006) 295.
8. A. Panda, Electrodeposition of nickel-copper alloys and nickel-copper-alumina nanocomposites into deep recesses for MEMS, (2003) Anna University, Chennai, India.
9. S. Budi, B. Kurniawan, D.M. Mott, S. Maenosono, A.A. Umar and A. Manaf, *Thin Solid Films.,* 642 (2017) 51.
10. W. Schwarzacher, *Electrochem. Soc. Interface.* 15 (2006) 32.
11. X. Ji, C. Yan, H. Duan and C. Luo, *Surf. Coatings Technol.,* 302 (2016) 208.
12. H.H. Lou, *Encycl. Chem. Process.,* (2006) 1. https://doi.org/10.1081/E-ECHP-120007747.
13. R.S. Bakdash, Codeposition of Copper-Zinc Alloy from Acidic Bath Containing Monosodium Glutamate, (2014) Taibah University, KSA.
14. S.S.A. El Rehim, M.A.M. Ibrahim and M.M. Dankeria, *J. Appl. Electrochem.*, 32 (2002) 1019.
15. R. Fukui, Y. Katayama and T. Miura, *Electrochim. Acta,* 56 (2011) 1190.
16. E.M. Oliveira, G.A. Finazzi and I.A. Carlos, *Surf. Coatings Technol.,* 200 (2006) 5978.

17. X. Zhao, X. Shang, Y. Quan, B. Dong, G.Q. Han, X. Li, Y.R. Liu, Q. Chen, Y.M. Chai and C.G. Liu, *Electrochim. Acta,* 230 (2017) 151.
18. J. Wang, Y. Wang, T. Xie and Q. Deng, *Mater. Lett.,* 245 (2019) 138.
19. Y. Wu, Y. Gao, H. He and P. Zhang, *Electrochim. Acta,* 301 (2019) 39.
20. K. Yao, M. Zhai and Y. Ni, *Electrochim. Acta,* 301 (2019) 87.
21. H. Liu, S. Zeng, P. He, F. Dong, M. He, Y. Zhang, S. Wang, C. Li, M. Liu and L. Jia, *Electrochim. Acta,* 299 (2019) 405.
22. M.A.M. Ibrahim, S.S.A. El Rehim, S.M.A. El Wahaab and M.M. Dankeria, *Plat. Surf. Finish.,* 86 (1999) 69.
23. M.A.M. Ibrahim and R.M. Al Radadi, *Chem. Phys.,* 151 (2015) 222.
24. M. Zamani, A. Amadeh and S.M.L. Baghal, *Trans. Nonferrous Met. Soc. China.,* 26 (2016) 484.
25. E. Barrera, M.P. Pardavé, N. Batina and I. González, *J. Electrochem. Soc.,* 147 (2000) 1787.
26. T.M. Manhabosco and I.L. Müller, *Surf. Coatings Technol.,* 202 (2008) 3585.
27. Y.L. Zhu, Y. Katayama and T. Miura, *Electrochim. Acta,* 55 (2010) 9019.
28. G. Cârâc and A. Ispas, *J. Solid State Electrochem.,* 16 (2012) 3457.
29. P. Yang, Y. Zhao, C. Su, K. Yang, B. Yan and M. An, *Electrochim. Acta*, 88 (2013) 203.
30. M.A.M. Ibrahim and R.M. Al Radadi, *Int J Electrochem Sci.,* 10 (2015) 4946.
31. U.S. Mohanty, B.C. Tripathy, P. Singh and S.C. Das, *J. Electroanal. Chem.,* 526 (2002) 63.
32. Y.L. Zhu, Y. Katayama and T. Miura, *Electrochim. Acta,* 85 (2012) 622.
33. M.A. El Sayed and M.A.M. Ibrahim, *Int. J. Electrochem. Sci.,* 14 (2019) 4957.
34. J. Guo, X. Guo, S. Wang, Z. Zhang, J. Dong, L. Peng and W. Ding, *Appl. Surf. Sci.,* 365 (2016) 31.
35. R.P. Oliveira, D.C. Bertagnolli, E.A. Ferreira, L. da Silva and A.S. Paula, *Surf. Coatings Technol.,* 349 (2018) 874.
36. A. Bahramian, M. Eyraud, F. Vacandio and P. Knauth, *Surf. Coatings Technol.,* 345 (2018) 40.
37. W. Wu, N. Eliaz and E. Gileadi, *Thin Solid Films.,* 616 (2016) 828.
38. B. Bozzini and L. D'Urzo, *Int. J. Electrochem. Sci.,* 4 (2009) 1028.
39. C. Lupi, A. Dell'Era and M. Pasquali, *Int. J. Hydrogen Energy,* 42 (2017) 28766.
40. J. Vijayakumar, S. Mohan, S.A. Kumar, S.R. Suseendiran and S. Pavithra, *Int. J. Hydrogen Energy,* 38 (2013) 10208.
41. Y.-Y. Yang and B. Deng, *Adv. Chem. Eng., Sci*., 1 (2011) 27.
42. M.A.M. Ibrahim and M. Messali, *Prod. Finish.*, 2 (2011) 14.
43. M.A.M. Ibrahim and E.M.A. Omar, *Surf. Coatings Technol.,* 226 (2013) 7.
44. R.M. Al Radadi and M.A.M. Ibrahim, *Korean J. Chem. Eng.,* 37 (2020) 1. https://doi.org/10.1007/s11814-020-0552-z.
45. M.A. Ibrahim and R.S. Bakdash, *Int. J. Electrochem. Sci.,* 10 (2015) 9666.
46. N.F. El Boraei and M.A.M. Ibrahim, *Surf. Coatings Technol.,* 347 (2018) 113.
47. I.M.A. Omar, M. Aziz and K.M. Emran, *Arab. J. Chem.,* (2020).
48. G. Barbato, Electrodeposition of tantalum and niobium using ionic liquid, (2009)
49. University of Toronto, Canada.
50. A.I. Alhaji, Electrodeposition of alloys from deep eutectic solvents, (2012) University of Leiceter, UK.
51. L. Anicai, A. Florea and T. Visan, Studies regarding the nickel electrodeposition from choline chloride based ionic liquids, *Appl. Ion. Liq. Sci. Technol.,* (2011) 261.
52. Z. Qibo and H. Yixin, Ionic Liquids as Electrodeposition Additives and Corrosion Inhibitors, in: Prog. Dev. Ion. Liq., InTech, (2017) National and University Library, Croatia.
53. Y. L. Zhu, Y. Katayama and T. Miura, *Electrochim. Acta,* 123 (2014) 303.
54. S. Wang, X. Guo, H. Yang, J. Dai, R. Zhu, J. Gong, L. Peng and W. Ding, *Appl. Surf. Sci.,* 288 (2014) 530.
55. S. Caporali, P. Marcantelli, C. Chiappe and C.S. Pomelli, *Surf. Coatings Technol.,* 264 (2015) 23.
56. S. Costovici, A.-C. Manea, T. Visan and L. Anicai, *Electrochim. Acta,* 207 (2016) 97.

57. R. Mardani, H. Shahmirzaee, H. Ershadifar and M.R. Vahdani, *Surf. Coatings Technol.,* 324 (2017) 281.
58. M.H. Allahyarzadeh, B. Roozbehani and A. Ashrafi, *Electrochim. Acta,* 56 (2011) 10210.